Simulating Bone Loss in Microgravity Using Mathematical Formulations of Bone Remodeling

James A. Pennline
Glenn Research Center, Cleveland, Ohio

NASA STI Program . . . in Profile

Since its founding, NASA has been dedicated to the advancement of aeronautics and space science. The NASA Scientific and Technical Information (STI) program plays a key part in helping NASA maintain this important role.

The NASA STI Program operates under the auspices of the Agency Chief Information Officer. It collects, organizes, provides for archiving, and disseminates NASA's STI. The NASA STI program provides access to the NASA Aeronautics and Space Database and its public interface, the NASA Technical Reports Server, thus providing one of the largest collections of aeronautical and space science STI in the world. Results are published in both non-NASA channels and by NASA in the NASA STI Report Series, which includes the following report types:

- TECHNICAL PUBLICATION. Reports of completed research or a major significant phase of research that present the results of NASA programs and include extensive data or theoretical analysis. Includes compilations of significant scientific and technical data and information deemed to be of continuing reference value. NASA counterpart of peer-reviewed formal professional papers but has less stringent limitations on manuscript length and extent of graphic presentations.

- TECHNICAL MEMORANDUM. Scientific and technical findings that are preliminary or of specialized interest, e.g., quick release reports, working papers, and bibliographies that contain minimal annotation. Does not contain extensive analysis.

- CONTRACTOR REPORT. Scientific and technical findings by NASA-sponsored contractors and grantees.

- CONFERENCE PUBLICATION. Collected papers from scientific and technical conferences, symposia, seminars, or other meetings sponsored or cosponsored by NASA.

- SPECIAL PUBLICATION. Scientific, technical, or historical information from NASA programs, projects, and missions, often concerned with subjects having substantial public interest.

- TECHNICAL TRANSLATION. English-language translations of foreign scientific and technical material pertinent to NASA's mission.

Specialized services also include creating custom thesauri, building customized databases, organizing and publishing research results.

For more information about the NASA STI program, see the following:

- Access the NASA STI program home page at *http://www.sti.nasa.gov*

- E-mail your question via the Internet to *help@ sti.nasa.gov*

- Fax your question to the NASA STI Help Desk at 443–757–5803

- Telephone the NASA STI Help Desk at 443–757–5802

- Write to:
  NASA Center for AeroSpace Information (CASI)
  7115 Standard Drive
  Hanover, MD 21076–1320

NASA/TM—2009-215824

Simulating Bone Loss in Microgravity Using Mathematical Formulations of Bone Remodeling

James A. Pennline
Glenn Research Center, Cleveland, Ohio

November 2009

Simulating Bone Loss in Microgravity Using Mathematical Formulations of Bone Remodeling

James A. Pennline
National Aeronautics and Space Administration
Glenn Research Center
Cleveland, Ohio 44135

Abstract

Most mathematical models of bone remodeling are used to simulate a specific bone disease, by disrupting the steady state or balance in the normal remodeling process, and to simulate a therapeutic strategy. In this work, the ability of a mathematical model of bone remodeling to simulate bone loss as a function of time under the conditions of microgravity is investigated. The model is formed by combining a previously developed set of biochemical, cellular dynamics, and mechanical stimulus equations in the literature with two newly proposed equations; one governing the rate of change of the area of cortical bone tissue in a cross section of a cylindrical section of bone and one governing the rate of change of calcium in the bone fluid. The mechanical stimulus comes from a simple model of stress due to a compressive force on a cylindrical section of bone which can be reduced to zero to mimic the effects of skeletal unloading in microgravity. The complete set of equations formed is a system of first order ordinary differential equations. The results of selected simulations are displayed and discussed. Limitations and deficiencies of the model are also discussed as well as suggestions for further research.

1.0   Introduction

Under the conditions of microgravity, astronauts lose bone mass and calcium (Ref. 1). In fact, bone can atrophy in space at a rate of about 1 percent a month, and some models suggest that a 40 to 60 percent total loss could eventually be reached (Ref. 13). Data from Buckley (Ref. 1) indicates that the greatest loss occurs in the lower extremities which experience the higher skeletal loadings during normal activity on earth. National Aeronautics and Space Administration (NASA) has a specific interest in understanding the mechanisms for bone loss during space flight for several reasons. Bone recovery has proven problematic. Based on a recovery model developed from medical data on astronauts who had flown on long duration missions (4 to 6 months), it could take as much as 9 months to recover 50 percent of the bone loss in some skeletal sites (Ref. 28). Other health hazards instigated by skeletal bone loss are accumulations of excess minerals in tissue such as the kidney, and increased risk of fracture. NASA is interested in developing interventions to sustain and protect the well being of its astronauts. Consequently, understanding bone loss is one of the research efforts being conducted for development of The Digital Astronaut. The Digital Astronaut is a an integrated, modular modeling and database system intended to support biomedical research to help identify and interpret medical and physiological research, to determine the effectiveness of specific human countermeasures to meet health and performance goals on exploration missions, and to evaluate medical interventions during mission emergencies, accidents, and illnesses (Ref. 24). Of particular concern is the effect on bone health from a longer duration mission such as a journey to Mars or the development of a Moon base. Existing measures of scheduled exercise with specially designed equipment may not be sufficient for preventing bone loss.

Bone remodeling is the process by which bone is removed and replaced on the same surface site by highly mediated and coupled action of bone cells. It's the physiological mechanism for enabling the normal maintenance of bone in the adult and is achieved by a balance between the processes of bone formation and bone resorption. These processes can be influenced by skeletal loading, endocrine regulation, and local biochemical mediators. Bone loss experienced by astronauts is thought to be caused by a disruption in the resorption-formation balance in favor of resorption, triggered by skeletal unloading.

Gravity is somehow converted from a mechanical signal to a chemical signal. Although much is known about the chemical signals, the process by which cells sense mechanical stimuli and then translate the information to a signal (mechanotransduction) that causes response within the cell or another cell, is not fully understood (Refs. 13 and 2).

Significant knowledge has been gained in understanding the biomechanical and molecular regulation of bone remodeling (Ref. 20). Work done in biomechanics has used mathematical formulations to describe how bone responds to stress and strain under loading. For example, in the study of fracture mechanics, mechanical and material properties are used to study how bones deform under loads. At the molecular and cellular level, building mathematical models of cellular dynamics has become an increasingly active research area in the last decade (Refs. 4, 5, 7, 8, 9, 14, 17, 19, 23, and 25). The cells that carry out the remodeling process are the *osteoclasts* that resorb bone by secretion of acid and proteases, and the *osteoblasts* that form bone by forming an initial collagen matrix (osteoid) and then mineralizing the collagen (Ref. 15). *Osteocytes*, matured osteoblasts encased in calcified bone matrix, are the cells that have been suggested to be the stimulus sensors or receptors of the stimulus signal. This suggestion is consistent with histologic and physiologic data (Ref. 2). One of the more descriptive models, which attempts to accurately detail the biochemical process, is the one by Lemaire et al. (Ref. 7). That model has also been used by other researchers as a base on which to build an extended model (Refs. 9, 14, and 17).

The majority of models in the literature lack some elements that prevent them from being used to model and simulate the effects of microgravity. In particular, there is a lack of a sufficient way to quantify bone loss or gain. The model in (Ref. 4) describes the change in bone density, as a percent, during a bone remodeling units cycle as a function of the change in the number of cells. Models in (Refs. 14 and 17) use similar representations of changes in relative mass. None of the others specify an explicit measure of bone loss or gain. Models also need to link the effect of the dynamics of loads on bone to the metabolic process. The model in (Ref. 9) is the first one this author has seen that attempts to combine how bone adapts to both cellular interactions and mechanical stimulus. It formulates the change in the intracortical radius of a cylindrical section of cortical bone under a force-induced stimulus that influences the cellular dynamic effects.

Most of the current cellular models focus on simulating the cause of specific bone diseases that occur on earth and the result of possible therapeutic strategies. The objective of this work is to investigate the applicability of some of the cellular dynamic models to NASA's interest in developing a model to help simulate the effects of microgravity and to provide quantitative analysis of bone mass and calcium levels to Digital Astronaut (DA). To do so we describe a model that uses the cellular dynamics from (Ref. 7), the force induced stimulus function from (Ref. 9), a new equation quantifying bone loss or gain, and an additional mass balance equation for calcium in bone fluid. In particular, the equation in (Ref. 9) that governs the changes in the intracortical thickness of a cylindrical section of cortical bone is replaced with an equation that governs the changes in the area of hard bone tissue in a cross section. The new equation can be related to the rate of change in the complement of bone porosity as defined in (Refs. 11 and 12). Section 2 gives a brief description of bone anatomy and the remodeling process. In Section 3, the physical part of the model is described and in Section 4, the model equations and variables are defined. In Section 5, the results of example simulations are discussed. Conclusions and recommendations for future research are made in Sections 6.

2.0   Bone Remodeling Process

The skeletal makeup includes cortical bone, the compact bone that forms the hard outside shell that encloses bone marrow, and trabecular (cancellous) bone, the spongy interior tissue in bone marrow. Trabecular bone is made up of a network of rod and plate like elements. Cortical bone is organized into Haversian systems, consisting of concentric layers of bone and a central canal (Haversian canal) which supplies blood. The boundaries between Haversian systems are referred to as cement lines. Within bone, osteocytes, cells derived from the bone forming cells, form what is understood to be a signaling network (Ref. 31).
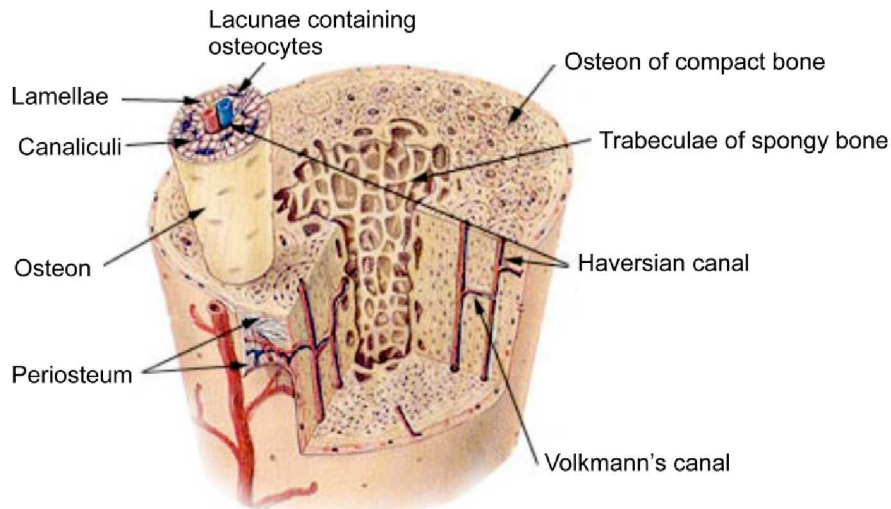
Figure 1.—Compact bone and spongy (cancellous bone).

Bone remodeling, the physiological mechanism for maintenance, renewal, and repair in the adult skeleton, is done threw the replacement of bone in units by the coupled action of bone cells on the same bone surface. The bone resorbing cells, osteoclasts, remove old or damaged bone. The bone forming cells, osteoblasts, form an initial collagen matrix and then mineralize the collagen. The replacement unit, often referred to as a basic multicellular unit (BMU) or bone remodeling unit (BRU), differs between trabecular bone and cortical bone. In trabecular bone the structural unit is a packet ideally shaped like a shallow crescent (hemi-osteon) on the surface of a rod or plate like element. In cortical bone the structural unit is a single Haversian system (Osteon) shaped like a cylinder and is referred to as a cutting cone while forming (Ref. 32).

The remodeling cycle of a BRU consists of 5 phases, activation, resorption, reversal, formation, and quiescence. Activation, the conversion of a small area of surface from quiescence to activity with respect to remodeling, requires recruitment of osteoclasts, a means for them to gain access to bone, and a mechanism for their attraction and attachment to the surface. Because of variations in age, sex, race, and metabolic state, and systematic differences between different bones and between different surfaces in the same bone, activation occurs sometimes at random and sometimes in response to focal events in the bone structure or biomechanical stimulus. In the normal adult skeleton it occurs about once every 10 sec (Ref. 15). Following activation, osteoclasts, proliferated from precursor cells, begin to erode a pit referred to as a Howship's lacuna in trabecular bone or burrow a tunnel called a cutting cone in cortical bone. (The pit characteristics were described in the previous paragraph.) The completion of resorption can take from one to three weeks. Reversal, the time interval between completion of resorption and beginning of formation at the same location, can last from one to two weeks. Formation by osteoblasts, derived from a different precursor cell, involves collagen matrix formation and mineralization. It lasts about three months, but it can take an additional several months for newly formed bone to become mature. Thus, the complete cycle is on the average about four months (Ref. 15). There are an estimated 10^5 to 10^6 active BRUs in the entire body at any one time (Ref. 33).

The processes of remodeling are controlled or influenced by hormones, protein receptors, ligands, other biochemicals, and mechanical stimulus. A complete description of the entire process of endocrine regulation, biochemical mediation, and stimulation by skeletal loading involved in bone remodeling is beyond the scope of this report. We shall briefly discuss the main substances involved in the cellular process that appear in the model equations of Section 4. The reader can refer to a list of their definitions in Appendix B. Early in the remodeling cycle, surface bound molecules, referred to as Receptor Activator for Nuclear Factor κB ligand (RANKL), are expressed on the surface of osteoblasts while the membrane protein Receptor Activator for Nuclear Factor κB (RANK) is expressed on the surface of preosteoclasts.

The binding of the receptor RANK with the ligand RANKL causes the derivation of active osteoclasts from preosteoclasts (Ref. 38). Parathyroid hormone (PTH), secreted by the parathyroid gland, is involved in promoting bone resorption by binding to osteoblasts and stimulating them to increase expression of RANKL. Thus PTH indirectly stimulates an increase in osteoclasts. PTH can have opposite effects on bone mass depending on whether it is released into the plasma continuously or on a pulsatory schedule (Ref. 5). Osteoprotegerin (OPG) is released by osteoblasts and acts as a decoy receptor for RANKL which blocks RANK-RANKL binding and inhibits preosteoclasts from maturing into active osteoclasts (Ref. 38). Transforming Growth Factor Beta (TGF-β) is released by osteoclasts during bone resorption. It has the ability to stimulate an increase of and activity in the osteoblast population, but it can also inhibit final maturation into active osteoblasts (Refs. 35 and 36). It's also thought to induce osteoclast apoptosis (Ref. 37). Nitric oxide, a gaseous signaling molecule, produced by osteoblasts directly regulates osteoclastic activity (Ref. 34). Prostaglandidn E2 (PGE$_2$) stimulates osteoblasts to release factors which stimulate resorption by osteoclasts. The model equations of Section 3 attempt to incorporate the effects of these substances.

3.0 Model Description

Current models for bone cell dynamics appearing in the literature of the last decade typically consist of three or more equations. The exact number can vary among models. Usually, there is one governing the rate of change in the population of the bone forming cells and one governing the rate of change in the population of the bone resorbing cells. There may or may not be equations for precursor cells and there may be equations for some or none of the biochemicals. In addition, the mathematical descriptions of the equations often differ among models. The reason for the difference in the number and form of the equations is due in part to the scientific assumptions used to create the equations. Some models are based more on biology (Refs. 5 and 7) while some are based more on experimental evidence (Refs. 4 and 21).

The physical domain in which the cellular dynamics is occurring and upon which the model is based varies among models. By physical domain, we mean the type, size, and skeletal location of bone used for numerical values of parameters and initial conditions of the model. For example, some models use a single BRU (Refs. 4 and 14). Others use an abstract small bone volume (Ref. 5), a section of bone whose BRUs are under the same external stimulus (Ref. 7), or a cylindrical section of a long bone (Ref. 9). Only a few of the models have an equation governing the rate of change of bone mass in the physical domain. In particular, the model of Komorova et al. (Ref. 4) and Moroz et al. (Ref. 14) include a rate equation for bone mass as a relative change from the initial value in units of percent. The model of Pivonka et al. (Ref. 17) includes an equation for relative change in bone volume in units of percent. Maldonado et al. (Ref. 9) use an equation in their model that governs the rate of change in the intracortical radius of a cylindrical section of cortical bone to quantify the amount of force induced bone gain. None of the other models referenced in the introduction have an equation governing the amount of bone gained or lost or the rate of change in the amount of bone. In those models, the gain in the population of active osteoblasts (loss in the population of active osteoclasts) or the gain in the population of active osteoclasts (loss in the population of active osteoblasts) is related to bone gain or loss, respectively.

In order to test a model's ability to simulate bone adaption in the environment of microgravity, the model must have a suitable quantification of bone mass at skeletal sites, and it must have a relation describing the bone mass as a function of time or an equation describing the rate of change of bone mass with time. In addition, the effect of mechanical stimulus and the contribution to bone balance from the normal skeletal loads on earth must be included.

This motivated the consideration of a model that combines the cellular dynamics model equations of Lemaire et al. (Ref. 7) with the mechanical stimulus equations in the model of Maldonado et al. (Ref. 9). The model in Reference 9 actually uses the cellular dynamics equations in Reference 7 coupled with a simple scalar description of a normal earth load on a segment of bone, but not an equation that governs bone mass explicitly. Their equation governing intracortical radius appears to have conflicting units because the rates of resorption and formation use values from the model of Komorova et al. which are in

units that are per cell whereas the rates in the model of Lemaire et al. are in units that are per pM concentration. The combined set of equations assemble here avoids conflicting units and attempts to model bone matrix lost or gained within a fixed radius.

According to a study of skeletal data obtained (up to 2007) by the U.S. and Russian space programs, trabecular bone loss on a percentage basis is greater than cortical bone loss in certain skeletal sites, but on a mass basis, the greatest loss is from cortical bone (Ref. 29). Therefore, the focus herein will be on quantifying the change in cortical bone.

Consider a simple model of a cylindrical section of cortical bone of cortical cross sectional area A and length L subject to a mean load F and stress given by

$$s = F / A \tag{3.1}$$

We will formulate the rate of change of bone area in the cortical region similar to the manner first described by Martin (Ref. 11) and further detailed in Reference 12. Figure 2(a) depicts a cross section containing secondary osteons or ORUs which are resorbing, refilling, or completed. Pathways of osteons may be irregular as well as regular and tunnel almost longitudinally but at a slight angle through the cortex (Ref. 12, p. 84). However it will be assumed that osteons and cutting cones of forming osteons are perpendicular to the cortical cross section and parallel to the axis of the cylindrical section of cortical bone. Therefore, within the cortical cross section there are cross sections of osteons. Figure 2(b) represents the cross section of a forming osteon. Martin defines a quantity called intracortical bone balance as

$$Q = Q_B N_F - Q_C N_R \tag{3.2}$$

where Q_B is the mean rate at which bone is replaced during refilling per osteon in mm^2/day, Q_C is the mean rate at which bone is resorbed in each osteon during its resorption phase, N_F is the number of osteons or BRUs forming bone per intracortical cross section A, and N_R is the number of BRUs resorbing bone per mm^2 cortex. Since resorption begins at the center of a Haversian system and ends at the cement line, and formation begins at the cement line and ends at the radius of the canal (Fig. 2(b)), these quantities are defined as

$$Q_B = \frac{\pi\left(R_c^2 - R_h^2\right)}{T_F}, \quad Q_C = \frac{\pi R_c^2}{T_R} \tag{3.3}$$

where R_c and R_h are the mean radius of an osteon's cement line and the mean radius of the Haversian canal, respectively. Quantities T_R and T_F represent the average time it takes for an osteon to complete its resorption phase and time to complete refilling phase, respectively. If f_a represents the activation frequency of a BRU, then in a dynamic situation where the normal remodeling balance is perturbed, f_a varies with time so that

$$N_F = \int_t^{t+T_F} f_a(s)ds, \, N_R = \int_t^{t+T_R} f_a(s)ds$$

If we assume that the activation frequency f_a of a BRU is constant (reasonable for bone in a steady state) then

$$N_F = f_a T_F, \quad N_R = f_a T_R \tag{3.4}$$

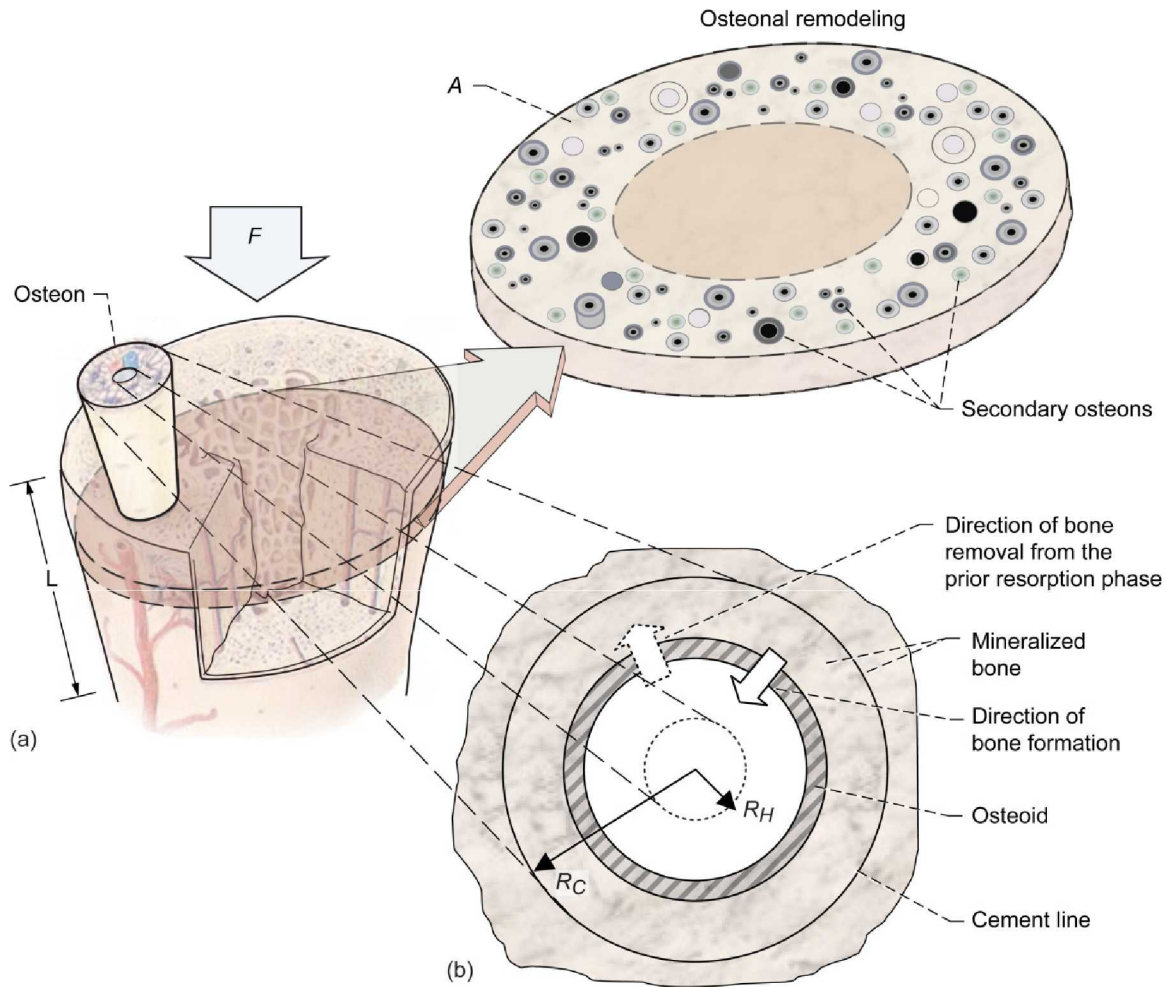and the times T_F and T_R will cancel out of Equation (3.2).

Figure 2.—(a) Sketch of the model. A cylindrical section of cortical bone carries a mean load F. It has a length L and cortical area A. A typical cross section contains Osteon remodeling units which are resorbing (resorption phase), refilling (formation phase) or completed. (b) Cross-sectional view of a refilling osteon (formation stage). The radius of the cement line is R_C. The radius of the Haversian canal is R_H. Formation starts at the cement line, fills inward, and stops at the radial distance of the Haversian canal thus creating an area equal to $\pi(R_C{}^2 - R_H{}^2)$. Prior to formation, the resorption phase removed a circular area of bone with radius R_C.

Actually, under constant f_a, Equation (3.2) would become a perfectly steady balance ($Q = 0$) by inserting the factor $(1-p)$ in the second term on the right hand side where

$$p = R_h^2 / R_c^2 \qquad (3.5)$$

Martin has suggested this alteration of the intracortical balance equation to account for osteons which eventually begin to overlap one another, which he has shown to limit porosity in sufficiently remodeled bone (Ref. 26). The value of p has been shown to be the upper limit on porosity when osteons are randomly located on the cross section (Ref. 26). To further define porosity, we note that the units of Q are mm^2 per day or $mm^2/A/day$ and if A_m denotes the area of hard bony matrix, the integral of Q over time is the amount of change in A_m. Then $A-A_m$, which we denote as A_v, is void area consisting of soft tissue. Consistent with Martin's definitions (Refs. 11 and 12) the quantity known as bone volume fraction would be

$$V_b = A_m / A \qquad (3.6)$$

and porosity would be

$$p_v = A_v / A \qquad (3.7)$$

A proposed equation for allowing changes in the normal bone balance Q or dA_m/dt and a proposed equation for the rate of change of calcium in bone fluid are coupled with the cellular dynamics equations (Ref. 7) and the mechanical stimulus equations (Ref. 9) to form the model equations.

4.0   Model Equations

The tables in Appendix A provide a definition of all the symbols used in this section. A common structure can be noted with many of these types of model equations. The rates of change of substances are constructed as a combination of accumulation terms and degradation terms. By accumulation (degradation) term we mean a term that increases (decreases) the substance rate of change. The system of equations here adopts a scheme in which rate coefficients are notated with a plus superscript if they act as an accumulation constant and a minus superscript if they act as degradation constant. The subscripts associate them with a specific substance. The current model equations are given by the system of equations assembled in tabular form below, followed by an explanation for each equation.

Rate of change of	Equation		Author(s)
Area of hard bone tissue	$\dfrac{dA_m}{dt} = Q_B N_F (\dfrac{B}{B_0}) - Q_C N_R (1 - p_v)(\dfrac{C}{C_0})$	(4.1A)	Pennline
Osteocyte concentration	$\dfrac{dO}{dt} = r_{BO}^+ (B - B_0) - r_{Oc}^- (O - O_0)$	(4.2)	
Nitric oxide concentration	$\dfrac{dK_{no}}{dt} = r_{no}^+ f_{bs} - r_{no}^- K_{no} + I_{no}$	(4.3)	Maldonado et al. (Ref. 9)
PGE$_2$ concentration	$\dfrac{dK_{pge}}{dt} = r_{pge}^+ f_{bs} + r_{(no)(pge)}^+ K_{no} - r_{pge}^- K_{pge} + I_{pge}$	(4.4)	
OPG concentration	$\dfrac{dK_O}{dt} = \dfrac{r_O}{E_P} B_R + I_O + r_{(no)(o)}^+ K_{NO} - r_O^- K_O$	(4.5)	
RANKL concentration	$\dfrac{dK_L}{dt} = r_L + I_L - r_{(no)(l)}^- K_{NO} - r_L \left(\dfrac{1 + (k_1/k_2)K_O + (k_3/k_4)K}{N_L E_P B} \right) K_L$	(4.6)	
Responding osteoblast concentration	$\dfrac{dB_R}{dt} = d_R E_G - \dfrac{0.05 d_B}{E_G} B_R + r_{(B)(pge)}^+ K_{pge}$	(4.7)	Lemaire et al. (Ref. 7)
Active osteoblast concentration	$\dfrac{dB}{dt} = \dfrac{0.05 d_B}{E_G} - k_B B$	(4.8)	
Active osteoclast concentration	$\dfrac{dC}{dt} = d_C E_R - d_A E_G C$	(4.9)	
Calcium concentration	$\dfrac{dCa}{dt} = -r_{FB}(B/B_0) + r_{BF}(C/C_0) + r_F + r_{CF} - r_{FC} - r_{dCa} Ca$	(4.10)	Pennline

The rate of change of $A_m(t)$ we propose is given by Equation (4.1A) where p_v is defined in Equation (3.7). This accounts for osteon overlap using Martin's factor discussed in Section 3. Note that it's modeled as a net gain or loss in cortical bone area (defined in Section 3) as a function of the ratio of change in cell level to normal cell level for both osteoblasts and osteoclasts. The effects of mechanical unloading (and loading) and biochemical imbalances are imposed through changes in cell populations caused by these effects. If an equation were used that is similar to the equation governing the rate of change of intra-cortical radius in (Ref. 9) it would look like the following

$$dA_m / dt = Q_B N_F (\frac{B}{B_0}) - Q_C N_R (\frac{C}{C_0}) + r_m^+ (\frac{O}{O_0}) - r_m^- (\frac{A_m}{A_{m0}}) \tag{4.1B}$$

where A_m replaces intra-cortical radius, $Q_B N_F$ replaces formation rate in radial direction, $Q_C N_R$ replaces resorption rate in radial direction, and r_m^+ and r_m^- are rate constants. Accumulation due to osteocytes from the third term is omitted in Equation (4.1A) since one could argue that osteocytes are derived from the osteoblasts. In comparison to Equations (4.1A), Equation (4.1B) will be shown to give incorrect results for bone loss.

Since the osteocyte concentration depends on the differentiation of the osteoblast population and the osteocytes are subject to cell death or apoptosis, an equation for the rate change of osteocyte concentration is given by Equation (4.2), where r_{BO}^+ and r_{Oc}^- are constant rates of differentiation and cell death, respectively.

Citing references that support their assumptions that osteocytes act as mechanosensors that cause the release of Nitrix Oxide (NO) and Prostaglandin E2 (PGE$_2$), Maldonado et al. (Ref. 9) define a nonlinear biochemical stimulus function of osteocyte concentration and stress. The biochemical stimulus function is given by

$$f_{bs}(s, O) = \frac{sO}{(1 + \exp(-(r_s s + r_{Oc} O)))} \tag{4.11}$$

where r_s and r_{Oc} are rate constants. The rates of change of NO and PGE$_2$ are then defined as a linear function of the biochemical stimulus and given by Equations (4.3) and (4.4) where r_{no}^+, r_{no}^-, r_{pge}^+, $r_{(no)(pge)}^+$, and r_{pge}^- are rate constants. The quantities I_{no} and I_{pge} represent injection inputs of NO and PGE$_2$, respectively.

Lemaire et al. (Ref. 7), describe a chemical kinetics analysis for RANKL, OPG, the binding complex of OPG-RANKL, and the RANK-RANKL complex. RANK is held fixed "to reflect the undiminished availability of osteoclast precursors". The four differential equations describing the rate of change of these quantities involving the cytokine RANKL and the receptors RANK and OPG are taken from (Ref. 6). From those equations Lemaire et al. (Ref. 7) obtain pseudo steady-state expressions for OPG and RANKL. In fact, if the steady-state expressions for the complexes OPG-RANKL and RANK-RANKL are substituted into the rate equations for RANKL and OPG, the result is Equations (4.5) and (4.6) where $r_{(no)(o)}^+$ is an accumulation constant, r_O^- and $r_{(no)(l)}^-$ are degradation constants, r_L is the rate of RANKL production and elimination, k_1/k_2 is the ratio of rates of OPG-RANKL binding/unbinding, and k_3/k_4 is the ratio of the rates of RANK-RANKL binding/unbinding. The constant N_L is the maximum number of RANKL attached on each cell surface, and r_O is the minimal rate of production of OPG per cell. Quantities I_O and I_L are injection rates of OPG and RANKL, respectively. The symbol E_P stands for PTH receptor occupancy ratio and is a function defined as

$$E_p(t) = \frac{I_P(t) + S_P}{I_P(t) + r_p^-(k_6/k_5)} \qquad (4.12)$$

where I_P is an injection rate of PTH, S_P is the rate of synthesis of systemic PTH, r_p^- is the rate of elimination of PTH, and k_6/k_5 is the ratio of rates of PTH unbinding/binding with its receptor.

To understand the formation of cell equations, the authors of (Ref. 7) state that their theory is based on the assumption that cell "proliferation" ("anti-proliferation") is proportional ("inversely proportional") to receptor occupancy (Ref. 7, p. 297). The equation governing the rate of change of responding osteoblasts is given by Equation (4.7), where d_R is a constant representing differentiation rate of osteoblast progenitors and E_G represents the fraction of occupied TGF-β receptors given by

$$E_G(t) = \frac{C(t) + 0.05C^S}{C(t) + C^S} \qquad (4.13)$$

The constant C^S represents the value of C to get half differentiation flux. By citing references that report that PGE$_2$ promotes bone formation, Maldonado et al. (Ref. 9) added the last term on the right hand side of Equation (4.7). It increases dB_R/dt by $r_{(B)(pge)}^+ K_{pge}$ where $r_{(B)(pge)}^+$ is a rate constant. Rates of change for the active osteoblasts and active osteoclasts are then described by Equations (4.8) and (4.9) where $E_R = (k_3/k_4)K_L$. The constants d_B, k_B, d_C, and d_A represent differentiation rate of responding osteoblasts, rate of elimination of active osteoblasts, differentiation rate of osteoclast precursors, and rate of osteoclast apoptosis caused by TGF-β, respectively. Note that the NO and PGE$_2$ dynamics is coupled to the RANK-RANKL-OPG dynamics to influence the osteoclast and osteoblast interactions through Equations (4.5) to (4.7).

Equation (4.10) is proposed for describing the rate of change of the concentration of calcium in the bone fluid and is based on a subset of a model by Jaros et al. (Ref. 3) involving the role of bone in calcium homeostasis. The symbols r_{FB}, r_{BF}, r_{CF}, and r_{FC} represent the rate of flow of calcium from bone fluid to bone, rate of flow of calcium from bone to bone fluid, rate of flow of calcium from blood capillary to bone fluid and rate of flow of calcium from bone fluid to blood capillary, respectively. The constant r_F represents the addition of calcium to the bone fluid from bone due to osteocytic osteolysis and is affected by the concentration of PTH (Ref. 3). The constant r_{dCa} represents a degradation of calcium due to an increased flow of calcium from bone fluid to blood capillary and is set to balance steady state for reference values of osteoclasts and osteoblasts. This also accounts for the fact that since an additional equation governing the concentration of calcium in the blood plasma is missing; the terms involving r_{CF} and r_{FC} are allowed to remain constant. Note that if the full model included an equation governing PTH concentration, an additional factor affecting the value of r_F would be included. The values for these constants are given in mmol per hour for the full skeleton. The units were converted to mmol per day and the values were scaled down. See Table 2.

Equations (4.1) to (4.10) constitute a coupled system of ten 1st order, ordinary differential equations. By specifying initial or steady-state values of the variables in Table 1, Equations (4.1) to (4.10) become an initial value, first-order system.

5.0   Simulation and Results

The quantities Q_B and Q_C for the formation and resorbtion rates were computed using human rib values for the mean Haversian canal and mean cement line radius from Polig and Jee (Ref. 18). An average value for activation frequency was computed from a range of rib values referenced by Martin (Ref. 11); while an average value of 20 mm^2 for cortical cross-sectional area, A, was chosen, using data from Abrams et al. (Ref. 39) which reports cortical area in the cross section of human ribs varying from

16.3 to 26.3 mm^2. The primary intent was to choose numerical values from some published data to be near correct orders of magnitude and not to choose cortical values from a specific long bone. They are not claimed to be the most accurate currently available. Based on what seemed to be about average normal values for the stress on long bones estimated using data from Buckley (Ref. 1, p. 16) on ranges of average values of the load in 1 g at various skeletal sites for a 70 kg body weight, a normal load (value of F) on earth on the order of 25 N was assumed for the cortical cross sectional area of 20 mm^2.

In Equations (4.3) and (4.4), f_{bs} was replaced by $(f_{bs}(s,O)-f_{bs}(25/20,O))$ (see Eq. 4.11). This was necessary in order to be consistent with the definition of the initial cell values for the equations from the model by Lemaire et al. (Ref. 7). Their parameter values of reference were selected to represent normal bone that is neither gaining nor losing mass, resulting in a system in a state of reference. Therefore, initial values from the Lemaire model must be assumed to be from bone with a normal physical load. This requires the combined equations to be in steady state when $F = 25$. Also, in Equations (4.1) to (4.10), we replaced the occurrence of each of the variables from Table 1 with the sum of its initial value plus a change. For example, $B(t)$ was replaced by $B(t)+B_0$, $C(t)$ was replaced by $C(t)+C_0$, and so on. Plots from simulations will then show the value of changes from the normal or steady state.

The method of solution of the equations was as follows. First, following the approach in (Ref. 9), Equations (4.3) to (4.6) were solved for their equilibrium expressions by assuming the rates of change are zero. This simplification was justified in both (Refs. 7 and 9) by stating that the binding reactions and chemical dynamics are much faster than the rest of the dynamics in the model. The expressions for NO, PGE$_2$, OPG, and RANKL are then substituted in the remaining equations where they appear. This left an initial value, first order system of six ODEs, consisting of Equations (4.1), (4.2), (4.7) to (4.10), which was numerically solved using a 4th order Runge-Kutta algorithm from Matlab. Unless stated otherwise in a specific simulation, the values used for the initial conditions, parameters, and constants are given in Tables 2 to 4 and correspond to values in References 7 and 9.

In reviewing the work of Lemaire et al. (Ref. 7), various bone diseases and possible therapies were simulated using their three cell equations. For example, since postmenopausal osteoporosis induced by estrogen deficiency is linked to a lack of OPG production (Ref. 27), they ran a simulation by decreasing r_O, the secretion rate of OPG by osteoblasts. They then tested a theoretical therapy by reducing k_B, the rate of elimination of active osteoblasts. In another example, they simulated the catabolic effect of continuous injection of PTH by running a simulation with I_P set to 1000 pM/day.

To check the agreement of the computations from the model Equations (4.1) to (4.10) with those of Lemaire et al. and the ability of the model to simulate bone disease on earth with no change in the normal force, a simulation with I_P set to 1000 pM/day was performed. Figure 3 shows the results wherein the normal load of ($F(t) = 25$) was used. This reduced Equations (4.7) to (4.9) to the same three cell equations employed in (Ref. 7) to give results for the osteoclasts and osteoblasts curves identical to those displayed in (Ref. 7, p. 300). The difference here is that simulation results showing the change in the area of hard bony tissue in the cortical cross section (lower right; Fig. 3) and the change in bone fluid calcium (lower left; Fig. 3) are displayed, whereas they are not displayed in (Ref. 7).

Note that the curve resulting from the use of (4.1B) shows an increase in bone area during the continuous injection period which is inconsistent with experimental and clinical observations (Ref. 30), whereas the response resulting from Equation (4.1A) shows the expected decrease in bone area. Actual values of the result from Equation (4.1B) were reduced by a factor of 10^{-1} to enable comparing the qualitative difference on the same plot.

In reviewing the use of their force-induced bone growth model, Maldonado et al. (Ref. 9) compared the difference between the effects of bone disease on the intracortical radius with physical activity and the effects without physical activity. They were able to show that physical activity is beneficial. For example, in the first test of their model they simulate the effects of an increased load on the intracortical radius. They ran a 350 day simulation during which the force F was increased on day 50 to mimic physical activity which increased their assumed average value of F to a value higher than the assumed normal
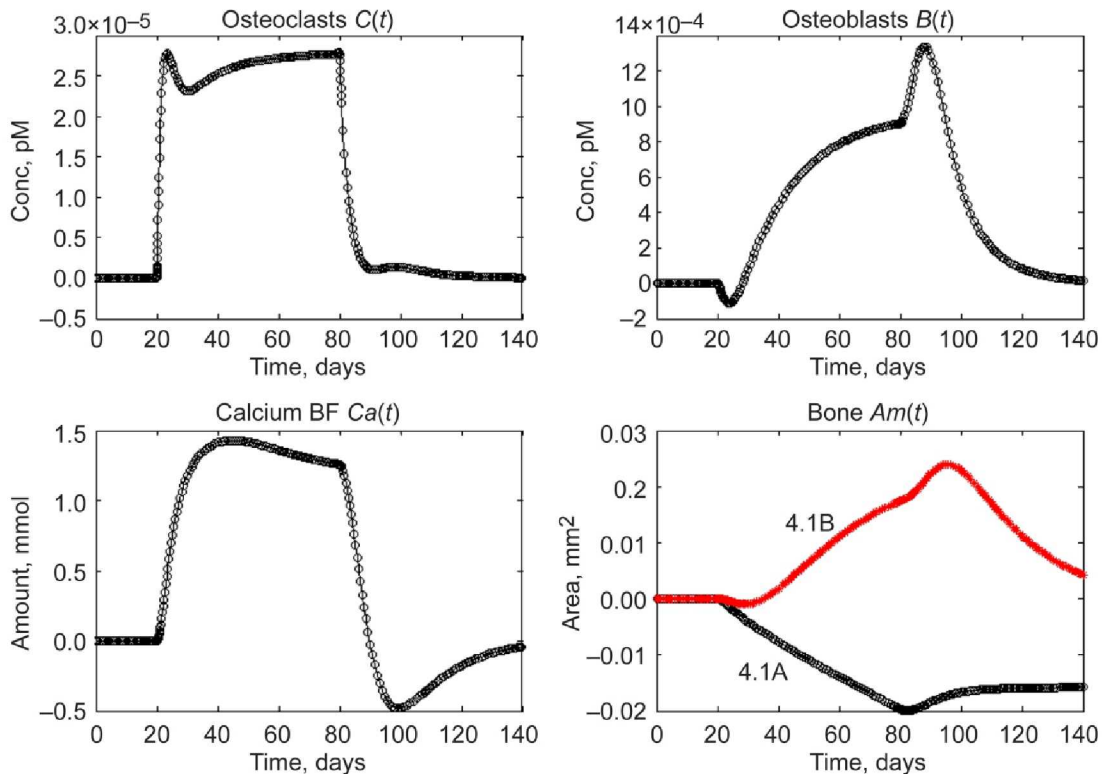
Figure 3.—Plots showing changes in osteoclasts, osteoblasts, bone fluid calcium, and bone area from a continuous injection (1000 pM/day) of PTH started on day 20 and then stopped on day 80.

value over the next 100 days. It was further increased on day 150. On day 250 the force was dropped to a value lower than the assumed normal value, to mimic a decrease in physical activity over next 100 days. The results show an increase in the radius between days 50 and 150 and another increase between days 150 and 250. The last one hundred days showed a decrease in the radius to a level slightly below the equilibrium value. A figure of those results can be seen in Reference 9.

For purpose of this study, a 350 day simulation of the model using Equation (4.1A) was conducted, where the load (value of F) was first decreased to zero on day 50. This would correspond to unloading the cylindrical section of bone upon entrance into the environment of microgravity on day 50. Figure 4 shows the results of such a simulation which also includes the bone area plot obtained using Equation (4.1B).

Once again, the response (change in bone area) resulting from the use of Equation (4.1A) predicts expected *qualitative* results in bone loss and gain. There is a continued loss of bone when the load is decreased to zero on day 50. On day 150 the average load is increased over the next 100 days, as the cumulative effects of physical activity is accounted for by increasing F to 20, and there is a decrease in the rate of loss of bone area, as shown. Corresponding to a return to 1 g on day 250, the load is increased above the normal load and bone loss begins to reverse.

On first glance, the response resulting from the use of Equation (4.1B) also indicates expected qualitative results in bone loss and gain in the following sense. Bone area in the cross section is lost in the interval of time beginning with a zero load. Raising the average load to 20 over an interval of time beginning on day 150 recovers some of the loss. Leaving the environment of a reduced load at day 250 and increasing the average load to 30 with physical activity recovers the lost bone area and then some. The shape of these curves is similar to the shape of the curves obtained in Reference 9 for bone growth induced by increasing the average force. However, it is not a good model of bone loss *in the environment of microgravity* where bone loss can continue over long periods of time, since the bone curve appears to level off or almost approach an asymptotic value in the unloaded interval ($F = 0$) without any countermeasure.
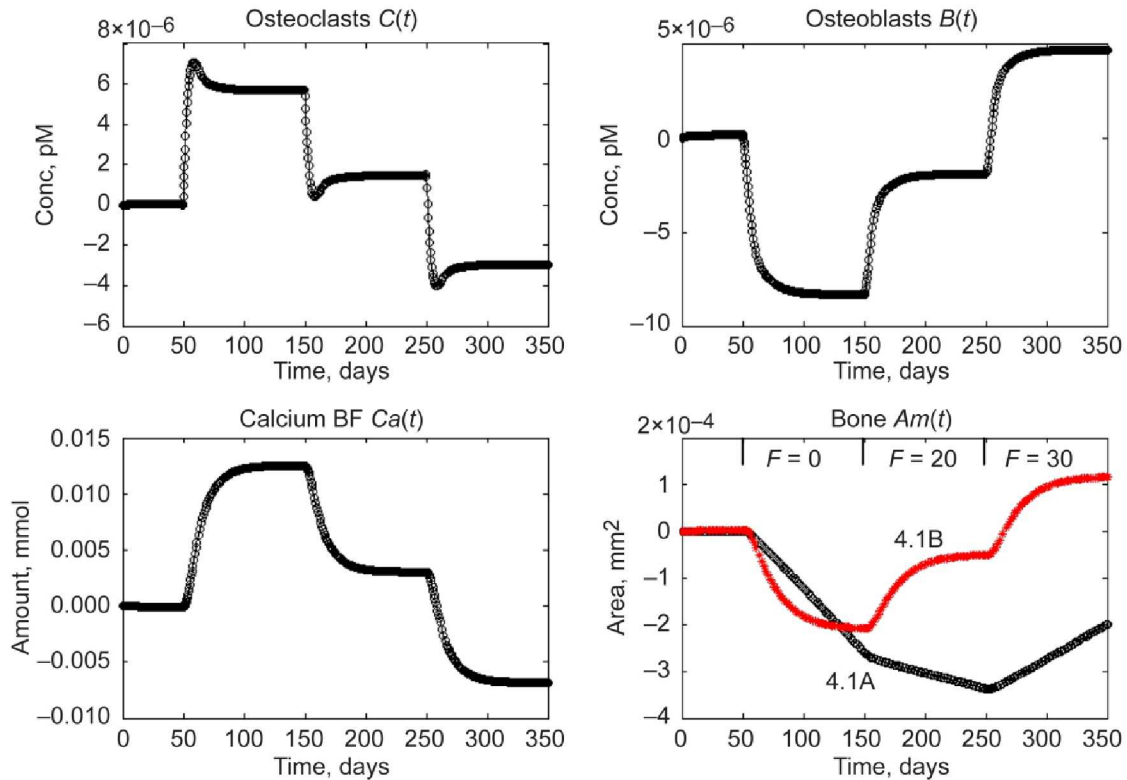
Figure 4.—Plots showing the changes in osteoclasts, osteoblasts, bone fluid calcium, and bone area obtained by setting $F = 0$ on day 50, increasing F to 20 on day 150, and then increasing the average load F to 30 on day 250.

Thus, the results of the present simulation demonstrate the following. The model Equation (4.1A) for rate of change of bone, which is more biologically accurate than Equation (4.1B), is able to more correctly simulate expected bone loss in microgravity which, in this model, means by reducing the normal value of F ($F = 25$) assumed on earth.

Biochemical imbalances under the conditions of microgravity may similarly cause disruptions in the bone remodeling balance in addition to those disruptions explained or modeled strictly by the mechanics of skeletal unloading. Lemaire et al. (Ref. 7) remark that osteoblast progenitors express TGF-β receptors so that TGF-β, produced by osteoclasts during bone resorption, leads to differentiation of the progenitors into responding osteoblasts. Using that knowledge, they associate bone loss, due to senescence on earth, with a decrease in the production of TGF-β. However, it is not clear what numerical values they modify to simulate bone loss due to senescence. We associated the consequence of senescence with one of the possible causes of old age osteoporosis, a decrease in the rate of osteoclast apoptosis due to TGF-β. Figure 5 shows the result of such a simulation of the model equations (without any skeletal unloading) using Equation (4.1A) for bone balance. Notice that when the osteoclast death rate due to TGF-β is reduced from 0.7 to 0.5 in the interval between day 20 and day 80, the loss of bone is similar to the loss in Figure 4 during the interval between day 50 and day 150. Bone area recovers and returns to the balanced state when the osteoclast death rate due to TGF-β is returned to its normal value.

It is of interest to examine the results of a simulation of this model that combines unloading with a reduction in the rate of osteoclast apoptosis due to TGF-β as a possible combination of bone remodeling imbalances in the environment of microgravity. Figure 6 shows the results of such a simulation using Equation (4.1A) for bone balance.
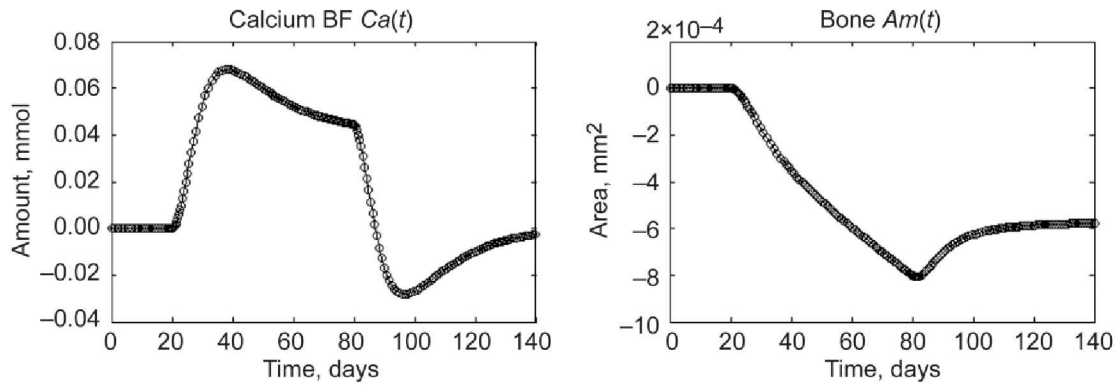
12

Figure 5.—Plots of bone fluid calcium in the section and bone area in the cross section. The value of d_A, the osteoclast death rate due to TGF-β, was reduced from 0.7 to 0.5 on day 20 and increased back to 0.7 on day 80. The simulation used Equation (4.1A).
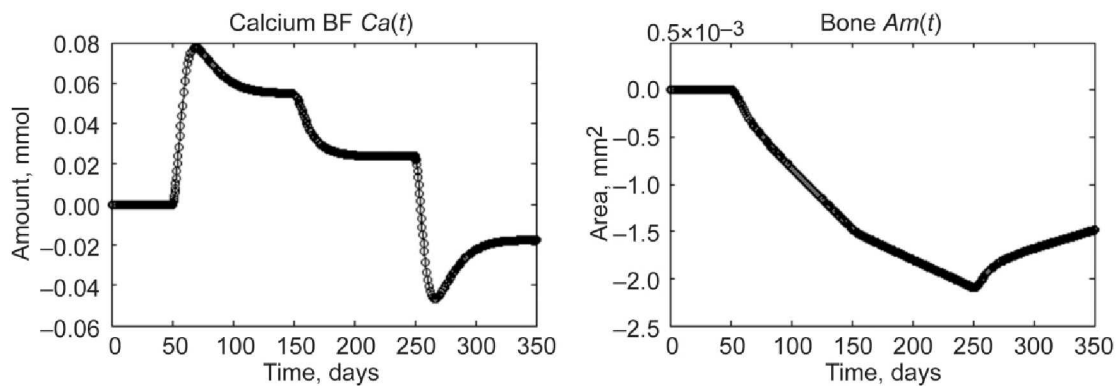

Figure 6.—Plots of changes in bone fluid calcium and bone area. Between day 50 and day 250 d_A, was reduced from 0.7 to 0.5. The load was set to 0 on day 50 and to 50.0 on day 150. On day 250, the load remained at 50.0 and d_A was restored to 0.7. The bone balance Equation (4.1A) was used.

Observe that the combined effects of reducing the rate of osteoclast apoptosis and unloading make it harder to recover bone loss with say physical activity that increases the average load. Increasing the average value of F above the normal load to 50.0 over the interval between day 150 and 250 still only showed a decrease in the rate of bone loss whereas without the added effect, bone loss would have been reversed. Other therapies and countermeasures besides increasing F could also be tested. However, we defer additional studies until a better model is developed, especially a model with a more robust description of the mechanical load on bone and mechanotransduction.

Conclusions

The simulations carried out with the simple model in this study show that mathematical formulations of the bone remodeling function could eventually be used for predicating bone loss in space. It is important that the model equations have a steady state or semi-steady state accurately perturbed by well-defined metabolic and biomechanical scenarios. However, to have a model with sufficient high fidelity to be used for application in the development of DA, or any other realistic simulations, much more research and development is needed. How bone loss or gain is quantified needs to be more accurately linked to the biological structure and remodeling phase of bone. Theories on the exact biomechanical stimulus for strain adaptation and mechanotransduction need to be more completely linked to the metabolic process. To be more specific, consider some of the limitations and flaws of the model in this study.

Although qualitative results look interesting, the modeling is still too abstract to be used for quantitative purposes, and this is true for other models in the literature. There is not enough dimensional

detail to be able to associate a collection of remodeling units under the same external stimulus with a specific location and size of bone segment. Our model does not include the complete set of cell types and biochemicals. For example, the interactions of phosphate ions are missing. The remodeling of trabecular bone is not addressed. The model here (and most other models) alters the resorption or formation rate based only on a change in the concentration of cells, and does not include a relation to changes in resorption depth or direction that Parfitt (Ref. 15, p. 73) associates with certain bone loss conditions. More research in needed in order to fully understand how the applied loads induce osteogenic response by various cell types in different regions (Ref. 16). Work is needed in designing experiments to quantify all model parameters and to insure unit and dimensional consistency, developing a benchmark for meeting requirements for realistic simulations, and developing validation tests.

References

1. Buckley Jr., J.C., Space Physiology, Oxford University Press, New York, 2006.
2. Cowin, S., The Exact Stimulus for the Strain Adaptation of Bone Tissue is Unknown, Journal of Biomechanical Science and Engineering, vol. 1, no. 1, pp. 16–28, 2006.
3. Jaros, G.G., Guyton, A.C., and Coleman, T.G. *The role of short-term calcium homeostasis: an analog-digital computer simulation*, Ann. Biomed. Eng., 8, pp. 103–141, 1980.
4. Komarova, S.V., Smith, R.J., Dixon, S.J., Sims, S.M., and Wahl, L.M. *Mathematical model predicts a critical role for osteoclast autocrine regulation in the control of bone remodeling*, Bone, 33, pp. 206–215, 2003.
5. Kroll, M.H. *Parathyroid hormone temporal effects on bone formation and resorption*, B. Math. Biology, 62, pp. 163–187, 2000.
6. Lauffenburger, D.A., and Linderman, J.J., Receptors: Models for Binding, Trafficking, and Signaling. Oxford University Press, New York; Toronto, 1996.
7. Lemaire, V., Tobin, F.L., Greller, L.D., Cho, C.R., and Suva, L.J. *Modeling interactions between osteoblasts and osteoclasts activities in bone remodeling*, J. Theoretical Biology, 229, pp. 293–309, 2004.
8. Maldonado, S., Borchers, S., Findeisen, R., and Allgower, F., Mathematical Modeling and Analysis of Force Induced Bone Growth, Proceedings of the 28th IEEE, EMBS Annual International Conference, New York City, USA, Aug. 30 to Sept. 3, 2006.
9. Maldonado, S., Findeisen, R., and Allgower, F., Phenomenological Mathematical Modeling and Analysis of Force-Induced Bone Growth and Adaptation, Proceedings of the FOSBE 2007, Stuttgart, Germany, Sept. 9–12, 2007.
10. Manolagas, S.C. *Choreography from the tomb: an emerging role of dying osteocytes in the purposeful and perhaps not so purposeful targeting of bone remodeling*, Osteovision, 3(1), pp. 5–14, 2006.
11. Martin, R.B., The Usefulness of Mathematical Models for Bone Remodeling, Yearbook of Physical Anthropology 28, pp. 227–236, 1985.
12. Martin, R.B., Burr, D.B., and Sharkey, N.A., Skeletal Tissue Mechanics, Springer-Verlag, New York, 1998.
13. Miller, K., *Gravity Hurts (So Good)*. (2001). Science@NASA, August 2, 2001. <http://science.nasa.gov/headlines/y2001/ast02sug_1.htm>.
14. Moroz, A., Crane, M.C., Smith, G., and Wimpenny, D.I., Phenomenological model of bone remodeling cycle containing osteocyte regulation loop, Biosystems 84, pp. 183–190, 2006.
15. Parfitt, A.M., Bone Remodeling: Relationship to Amount and Structure of Bone, and the Pathogenesis and Prevention of Fractures, Osteoporosis: Etiology, Diagnosis, and Management, edited by H. Lawrence Riggs and L. Joseph Melton, III., Raven Press, New York, 1988.
16. Pearson, O.M. and Lieberman, D.E., The Aging of Wolff's "Law": Ontogeny and Responses to Mechanical Loading in Cortical Bone, Yearbook of Physical Anthropology, 47, pp. 63–99, 2004.

17. Pivonka, P., Simak, J., Smith, D.W., Gardiner, B.S., Dunstan, C.R., Sims, N.A., Martin, T.J., and Mundy G.R., Model Structure and Control of Bone Remodeling: A Theoretical Study, Bone 43, pp. 249–263, 2008.

18. Polig, E., and Jee, W.S.S., A Model of Osteon Closure in Cortical Bone, Calcified Tissue International, 47, pp. 261–269 1990.

19. Rattanakul, C.R., Lenbury, Y., Krishnamara, N., and Wolkind, D.J. *Modeling of bone formation and resorption mediated by parathyroid hormone: resonse to estrogen/PTH therapy*, BioSystems, 70, pp. 55–72, 2003.

20. Robling, A.G., Castillo, A.B., and Turner, C.H. *Biomechanical and molecular regulation of bone remodeling*, Annu. Rev. Biomed. Eng., 8, pp. 455–498, 2006.

21. Ruimerman, R., van Reitbergen, B., Hilbers P., and Huiskes, R. *A 3-dimensional computer model to simulate trabecular bone metabolism*, Biorheology, 40, 315–320, 2003.

22. Talmage, R.V. and Myer Jr., R.A. *Physiological role of parathyroid hormone*, In Handbook of Physiology, vol. III Endocrinology, G.D. Aurbach (Ed.) American Physiological Society, Washington D.C., pp. 343–351, 1976.

23. Wang Z., Song, W., Li, Y., Dhar, P., Tsuchiya, M., and Mondry, A., Quantitative study of calcium homeostasis maintenance through systemic modeling, FOSBE 2005, Santa Barbara, California, USA, August 2005.

24. White, R.J. and McPhee, J.C., The Digital Astronaut: An integrated modeling and database system for space biomedical research and operations, 60, pp. 273–280, 2007.

25. Wimpenny, D.I., and Moroz, A., On allosteric control model of bone turnover cycle containing osteocyte regulation loop, Biosystems 90, pp. 295–308, 2007.

26. Martin, R.B., Overlap feedback: An autonomous mechanism for controlling porosity during haversian bone remodeling, Proceedings, Fourth Annual New England Bioengineering Conference, New Haven, CT, pp. 41–44, 1976.

27. Hofbauer, L.C., Khosla, S., et al., Estrogen stimulates gene expression and protein production of osteoprotegerin in human osteoblastic cells, Endocrinology 140 (9), 4367–4370, 1999.

28. Sibonga, J.D., and et al., Recovery of spaceflight-induced bone loss: Bone mineral density after long-duration missions as fitted with an exponential function, Bone 41, 973–978, 2007.

29. LeBlanc, A.D., et al., Skeletal responses to space flight and the bed rest analog: A review, J Musculoskelet Neuronal Interact 7 (1), 33–47, 2007.

30. Watson, P.H., Fraher, L.J., et al., enhanced osteoblast development after continuous infusion of hPTH(1-84) in the rat, Bone 24 (2), 89–94, 1999.

31. Bone Structure and Function, ASBMR Bone Curriculum, Susan Ott website <http://depts.washington.edu/bonebio/ASBMRed/structure.html>

32. Bronner, F. and Worrell, R., Orthopaedics: principles of basic and clinical science, CRC Press LLC, 1999.

33. Langton, C.M. et al., Dynamic stochastic simulation of cancellous bone resorption, Bone, vol. 22, no. 4, 1998.

34. Evans D.M., Ralston S.H., Nitric oxide and bone, J. Bone Miner Res. Mar; 11(3):300-5. 1996.

35. Bonewald, L.F. and Dallas, S.L., Role of active and latent TGF-β in bone formation, J. Cell. Biochem. 55(3), 350–357, 1994.

36. Alliston, T. and Choy, L., et al., TGF-β-induced repression of CBFA1 by Dmad3 decreases cbfal and osteocalcin expression and inhibits osteoblast differentiation, Embo J. 20 (9), 2254–2272, 2001.

37. Roodman, G.D., Cell biology of the osteoclast, Exp. Hematol, 27 (8), 1299–1241, 1999.

38. Hofbauer, L.C., Khosla, S., et al., The roles of osteoprotegerin and osteoprotegerin ligand in the paracrine regulation of bone resorption, J. Bone Mineral Res. 15 (1), 2–12, 2000.

39. Abrams, E., Mohr, M. et al., Cross-Sectional Geometry of Human Ribs, Legacy Clinical Research & Technology Center Report, Portland, OR., 2000.

Appendix A.—Tables

TABLE 1.—NOMENCLATURE

Symbol	Definition	Unit
$A_m(t)$	Area of bone	mm^2
$B(t)$	Concentration of osteoblasts	pM
$B_R(t)$	Concentration of responding osteoblasts	pM
$C(t)$	Concentration of osteoclasts	pM
$O(t)$	Concentration of osteocytes	pM
$Ca(t)$	Calcium concentration	mmol
$K_L(t)$	Concentration of RANKL	pM
$K_{no}(t)$	Concentration of nitric oxide	pM
$K_O(t)$	Concentration of osteoprotegerin (OPG)	pM
$K_{pge}(t)$	Concentration of prostaglandin E_2 (PGE_2)	pM
$I_L(t)$	Injection rate of RANKL	pM/day
$I_{no}(t)$	Injection rate of nitric oxide	pM/day
$I_O(t)$	Injection rate of OPG	pM/day
$I_P(t)$	Injection rate of PTH	pM/day
$I_{pge}(t)$	Injection rate of PGE_2	$pM\ day^{-1}$

TABLE 2.—INITIAL VALUES

Symbol	Value	Definition
A_{m0}	$18\ mm^2$	Initial value bone area
B_0	0.0007282 pM	Initial value active osteoblasts
B_{R0}	0.0007734 pM	Initial value responding osteoblasts
C_0	0.0009127 pM	Initial value active osteoclasts
C	0.0073 pM	Initial value osteocytes
Ca_0	0.696 mmol	Initial value calcium (Bone fluid)

TABLE 3.—PARAMETER VALUES

Symbol	Value	Definition
$Q_B N_F$	0.173×10^{-3} mm^2 day^{-1}	Rate of formation of bone area by osteoblasts
$Q_C N_R$	0.156×10^{-3} mm^2 day^{-1}	Rate of resorption of bone area by osteoclasts
r_m^+	1.0 mm^2 day^{-1}	Rate of increase of bone area due to osteocytes
r_m^-	1.0 day^{-1}	Rate of degradation of bone area
r_{BO}^+	0.1 day^{-1}	Osteocyte production rate from differentiation of osteoblasts
r_{Oc}^-	1 day^{-1}	Osteocyte degradation rate
r_s	1 mm^2/N	Stress influence rate
r_{Oc}	1.0 pM^{-1}	Osteocyte influence rate
r_{no}^+	2.0×10^4 mm^{2}day/N	Rate of release of NO
r_{no}^-	1.0×10^3 day^{-1}	NO elimination rate
r_{pge}^+	100 mm^{2}day/N	Rate of release of PGE$_2$ due to biochemical stimulus
$r_{(no)(pge)}^+$	1.0 day^{-1} or 10.0 day^{-1}	PGE$_2$ rate increased by NO
r_{pge}^-	1.0×10^2 day^{-1}	PGE$_2$ elimination rate
$\underline{r_O}$	2×10^5 pmol day^{-1}/pmol cells	Minimal rate of production of OPG per cell
$r_{(no)(o)}^+$	10 day^{-1}	OPG rate increase by NO
r_O^-	0.35 day^{-1}	Rate of elimination of OPG
r_L	10^3 pM day^{-1}	Rate of RANKL production and elimination
$r_{(no)(l)}^-$	100 day^{-1}	RANKL rate decreased by NO
r_p^-	86 day^{-1}	Rate of elimination of PTH
$r_{(B)(pge)}^+$	1.0×10^{-4} day^{-1}	B_R rate increased by PGE$_2$

TABLE 4.—PARAMETER VALUES

Symbol	Value	Definition
C^S	5×10^{-3} pM	Value of C to get half differentiation flux
d_A	0.7 day^{-1}	Rate of osteoclast apoptosis caused by TGF β
d_B	0.7 day^{-1}	Differentiation rate of responding osteoblasts
d_C	2.1×10^{-3} pM day^{-1}	Differentiation rate of osteoclast precursors
d_R	7×10^{-4} pM day^{-1}	Differentiation rate of osteoblast progenitors
K	10 pM	Fixed concentration of RANK
k_1	10^{-2} pM^{-1}day^{-1}	Rate of OPG-RANKL unbinding
k_2	10 day^{-1}	Rate of OPG-RANKL unbinding
k_3	5.8×10^{-4} pM^{-1}day$^-$	Rate of RANK-RANKL binding
k_4	1.7×10^{-2} day^{-1}	Rate of RANK-RANKL unbinding
k_5	0.02 pM^{-1}day^{-1}	Rate of PTH binding with its receptor
k_6	3 day^{-1}	Rate of PTH unbinding
N_L	3×10^6 pmol/pmol cells	Maximum number of RANKL attached on each cell surface
k_B	0.189 day^{-1}	Rate of elimination of active osteoblasts
r_{FB}	0.072 mmol day^{-1}	Rate of flow of calcium from bone fluid to bone
r_{BF}	0.0696 mmol day^{-1}	Rate of flow of calcium from bone to bone fluid
r_{CF}	1.2696 mmol day^{-1}	Rate of flow of calcium from blood capillary to bone fluid
r_{FC}	1.2 mmol day^{-1}	Rate of flow of calcium from bone fluid to blood capillary
r_F	0.0024 mmol day^{-1}	Rate of accumulation of calcium in bone fluid due to osteocytic osteolysis
r_{dCa}	0.1 day^{-1}	Calcium degradation rate

Appendix B.—Substance Definitions

Unless specifically referenced, definitions were taken from Wikipedia, The Free Encyclopedia, http://en.wikipedia.org/wiki/.

1. Receptor.—A protein molecule, embedded in either the plasma membrane or cytoplasm of a cell, to which a mobile signaling molecule may attach.
2. Ligand.—A molecule that binds to a receptor.
3. Receptor Activator of Nuclear Factor κ B (RANK).—Membrane protein which is expressed on the surface of osteoclasts and is involved in the activation of osteoclasts upon ligand binding.
4. Receptor Activator for Nuclear Factor κ B Ligand (RANKL).—A surface bound molecule expressed on osteoblasts that stimulates osteoclast differentiation from preosteoclasts through binding with RANK.
5. Parathyroid Hormone (PTH).—A hormone secreted by parathyroid gland that enhances release of calcium from bone and indirectly stimulates osteoclasts by binding to osteoblasts which in turn stimulates osteoblasts to increase expression of RANKL.
6. Osteoprotegerin (OPG).—A decoy receptor for RANKL that prevents osteoclast maturation by blocking the RANKL-RANK interaction.
7. Transforming Growth Factor beta (TGF-β).—Controls cellular differentiation and other functions in most cells and induces apoptosis in numerous cell types. TGF-β is released by osteoclasts during bone resorption. It has the ability stimulate addition in and activity in the preosteoblast population but it can also inhibit final maturation into active osteoblasts (Refs. 35 and 36). It's also known to induce osteoclast apoptosis (Ref. 37).
8. Nitric Oxide (NO).—A gaseous signaling molecule produced by osteoblasts which directly regulates osteoclastic activity (Ref. 34).
9. Prostaglandin E2 (PGE$_2$).—A substance that stimulates osteoblasts to release factors which stimulate bone resorption by osteoclasts.

1. REPORT DATE (DD-MM-YYYY) 01-11-2009	2. REPORT TYPE Technical Memorandum	3. DATES COVERED (From - To)

4. TITLE AND SUBTITLE Simulating Bone Loss in Microgravity Using Mathematical Formulations of Bone Remodeling	5a. CONTRACT NUMBER
	5b. GRANT NUMBER
	5c. PROGRAM ELEMENT NUMBER
6. AUTHOR(S) Pennline, James, A.	5d. PROJECT NUMBER
	5e. TASK NUMBER
	5f. WORK UNIT NUMBER WBS 516724.02.02.08.01

7. PERFORMING ORGANIZATION NAME(S) AND ADDRESS(ES) National Aeronautics and Space Administration John H. Glenn Research Center at Lewis Field Cleveland, Ohio 44135-3191	8. PERFORMING ORGANIZATION REPORT NUMBER E-17086

9. SPONSORING/MONITORING AGENCY NAME(S) AND ADDRESS(ES) National Aeronautics and Space Administration Washington, DC 20546-0001	10. SPONSORING/MONITOR'S ACRONYM(S) NASA
	11. SPONSORING/MONITORING REPORT NUMBER NASA/TM-2009-215824

12. DISTRIBUTION/AVAILABILITY STATEMENT
Unclassified-Unlimited
Subject Categories: 52, 59, and 64
Available electronically at http://gltrs.grc.nasa.gov
This publication is available from the NASA Center for AeroSpace Information, 443-757-5802

13. SUPPLEMENTARY NOTES

14. ABSTRACT
Most mathematical models of bone remodeling are used to simulate a specific bone disease, by disrupting the steady state or balance in the normal remodeling process, and to simulate a therapeutic strategy. In this work, the ability of a mathematical model of bone remodeling to simulate bone loss as a function of time under the conditions of microgravity is investigated. The model is formed by combining a previously developed set of biochemical, cellular dynamics, and mechanical stimulus equations in the literature with two newly proposed equations; one governing the rate of change of the area of cortical bone tissue in a cross section of a cylindrical section of bone and one governing the rate of change of calcium in the bone fluid. The mechanical stimulus comes from a simple model of stress due to a compressive force on a cylindrical section of bone which can be reduced to zero to mimic the effects of skeletal unloading in microgravity. The complete set of equations formed is a system of first order ordinary differential equations. The results of selected simulations are displayed and discussed. Limitations and deficiencies of the model are also discussed as well as suggestions for further research.

15. SUBJECT TERMS
Bone remodeling; Mathematical model; Microgravity; Bone demineralization; Differential equations; Simulation

16. SECURITY CLASSIFICATION OF:			17. LIMITATION OF ABSTRACT	18. NUMBER OF PAGES	19a. NAME OF RESPONSIBLE PERSON STI Help Desk (email:help@sti.nasa.gov)
a. REPORT U	b. ABSTRACT U	c. THIS PAGE U	UU	25	19b. TELEPHONE NUMBER (include area code) 443-757-5802